Electronic Supplementary Material (ESI) for ChemComm.
This journal is © The Royal Society of Chemistry 2021

Supporting Information

# Multi-component Synthesis of Dihydro-1,3-azaborinine Derived Oxindole Isosteres

Jun Li, Constantin G. Daniliuc, Jonas Matern, Gustavo Fernández, Gerald Kehr and Gerhard Erker*

## Content

Experimental Procedures ..... 2
Preparation of compound **4a** ..... 3
Preparation of compound **4b** ..... 6
Preparation of compound **4c** ..... 10
Preparation of compound **4d** ..... 13
Photophysical properties ..... 16
General Procedures ..... 16
Fluorescence emission and excitation spectroscopy ..... 16
Fluorescence quantum yields ..... 20
References ..... 21

## Experimental Procedures

**General Information.** All reactions involving air- or moisture-sensitive compounds were carried out under an inert gas atmosphere (Argon) by using Schlenk-type glassware or in a glovebox. All solvents were dried and degassed before use, if necessary, for the respective reaction. Chemicals: Unless otherwise noted all chemicals were used as purchased. The following instruments were used for physical characterization of the compounds: elemental analyses: Foss–Heraeus CHNO-Rapid; HRMS: Thermo Scientific Orbitrap LTQ XL; NMR: Varian UNITY plus NMR spectrometer ($^{1}$H, 600 MHz; $^{13}$C, 151 MHz; $^{11}$B, 192 MHz; $^{19}$F, 564 MHz). $^{1}$H and $^{13}$C NMR chemical shifts are given relative to tetramethylsilane (TMS) and referenced to the solvent signal. $^{19}$F and $^{11}$B are referenced according to the proton resonance of TMS as the primary reference for the unified chemical shift scale (IUPAC recommendation 2001: R. K. Harris, E. D. Becker, S. M. Cabral De Menezes, R. Goodfellow, P. Granger, *Pure Appl. Chem.* 2001, **73**, 1795-1818]. NMR assignments were supported by 2D NMR experiments.

X-Ray diffraction: Data sets for compounds **4a**, **4b** and **4c** were collected with a Bruker D8 Venture CMOS diffractometer. Programs used: data collection: APEX3 V2016.1-0 (Bruker AXS Inc., **2016**); cell refinement: SAINT V8.37A (Bruker AXS Inc., **2015**); data reduction: SAINT V8.37A (Bruker AXS Inc., **2015**); absorption correction, SADABS V2014/7 (Bruker AXS Inc., **2014**); structure solution *SHELXT-2015* (Sheldrick, G. M. *Acta Cryst.,* **2015**, *A71*, 3-8); structure refinement *SHELXL-2015* (Sheldrick, G. M. *Acta Cryst.,* **2015**, *C71* (1), 3-8). *R*-values are given for observed reflections, and *w*R$^2$ values are given for all reflections. *Exceptions and special features*: For compound **4b** three $CF_3$ groups and for compound **4c** two $CF_3$ groups and two thiophene groups were found disordered over two positions in the asymmetric unit. Several restraints (SADI, SAME, ISOR and SIMU) were used in order to improve refinement stability.

Materials: Borane **7** was prepared according to a procedure described in the literature.[4]

Numbering of the azaborinine ring for the assignment of NMR signals:

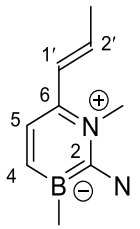

## Preparation of compound 4a

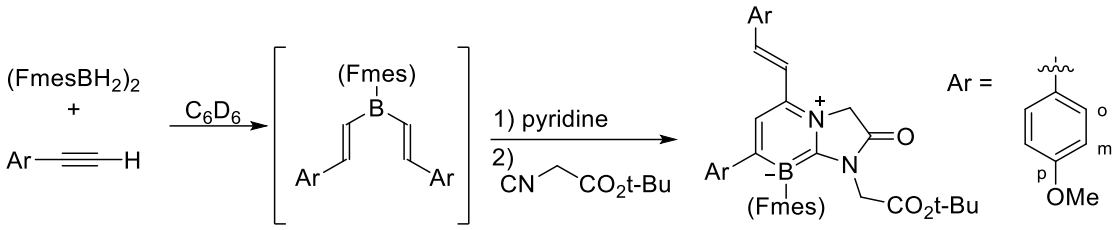


Scheme S1

At room temperature, 1-ethynyl-4-methoxybenzene (52.8 mg, 0.4 mmol, 2 equiv.) was added to a suspension of borane **7** ([[$FmesBH_2)_2$] 58.8 mg, 0.1 mmol, 1 equiv.) in $C_6D_6$ (1 mL). The mixture was stirred at room temperature for 30 min to give a yellow solution. Pyridine (79 mg, 1 mmol, 5 equiv.) was added to the solution and stirred for 5 min. Then isocyanide **8** (56.4 mg, 0.4 mmol, 2 equiv.) in $C_6D_6$ (1 mL) was added to the solution. The resulting mixture was stirred for 2 days. All the volatiles were removed in vacuum. The residue was purified via chromatography of silica gel with pentane: ethyl acetate (7 : 1) as eluents to give the compound **4a** as yellow solid (96 mg, 63 % yield).

**HRMS** for $C_{37}H_{32}BF_9N_2O_5^+$ ($M^+$): Calc. (766.2262), Found: 766.2272.

**$^1$H NMR** (600MHz, methylene chloride-$d_2$, 299 K): δ = 8.13 (s, 2H, *m*-Fmes), 7.67 (s, 1H, C(5)H), 7.50 (m, 2H, *o*-*p*-Anisole$^{(2')}$), 7.23 (d, $^3J_{HH}$ = 15.8 Hz, 1H, C(2')H), 6.94 (m, 4H, *m*-*p*-Anisole$^{(2')}$, *o*-*p*-Anisole$^{(4)}$), 6.85 (d, $^3J_{HH}$ = 15.8 Hz, 1H, C(1')H), 6.68 (m, 2H, *m*-*p*-Anisole$^{(4)}$), 4.92 (s, 2H, $CH_2^{(1)}$), 3.84 (s, 3H, *p*-$OCH_3^{p\text{-Anisole}(2')}$), 3.73 (s, 2H, $CH_2^{N(2)}$), 3.72 (s, 3H, *p*-$OCH_3^{p\text{-Anisole}(4)}$), 1.30 (s, 9H, $CH_3^{t\text{-Bu}}$).

**$^{13}$C{$^1$H} NMR** (151 MHz, methylene chloride-$d_2$, 299 K): δ = 168.4 (NC=O), 165.4 (OC=O), 160.7 (*p*-*p*-Anisole$^{(2')}$), 158.5 (*p*-*p*-Anisole$^{(4)}$), 156.9 (br, C(4)), 152.9 (br, C(2)), 147.8 (br, *i*-Fmes), 138.4 (*i*-*p*-Anisole$^{(4)}$), 136.0 (q, $^2J_{FC}$ = 29.6 Hz, *o*-Fmes), 132.5 (C(2')H), 131.3 (br, C(6)), 130.7 (q, $^2J_{FC}$ = 34.2 Hz, *p*-Fmes), 129.45 (*o*-*p*-Anisole$^{(4)}$), 129.39 (*i*-*p*-Anisole$^{(2')}$), 128.6 (*o*-*p*-Anisole$^{(2')}$), 126.2 (br m, *m*-Fmes), 123.83 (q, $^1J_{FC}$ = 274.8 Hz, *o*-$CF_3$), 123.80 (C(5)H), 123.5 (q, $^1J_{FC}$ = 271.8 Hz, *p*-$CF_3$), 117.4 (C(1')H), 114.7 (*m*-*p*-Anisole$^{(2')}$), 113.6 (*m*-*p*-Anisole$^{(4)}$), 82.8 ($C^{t\text{-Bu}}$), 55.7 (*p*-$OCH_3^{p\text{-Anisole}(2')}$), 55.4 (*p*-$OCH_3^{p\text{-Anisole}(4)}$), 52.3 ($CH_2^{(1)}$), 44.2 ($CH_2^{N(2)}$), 27.9 ($CH_3^{t\text{-Bu}}$).

**$^{11}$B{$^1$H} NMR** (192 MHz, methylene chloride-$d_2$, 299 K): δ = 23.8 ($v_{1/2}$ ≈ 400 Hz).

**$^{19}$F NMR** (564 MHz, methylene chloride-$d_2$, 299 K): δ = -59.2 (s, 2F, *o*-$CF_3$), -63.4 (s, 1F, *p*-$CF_3$).

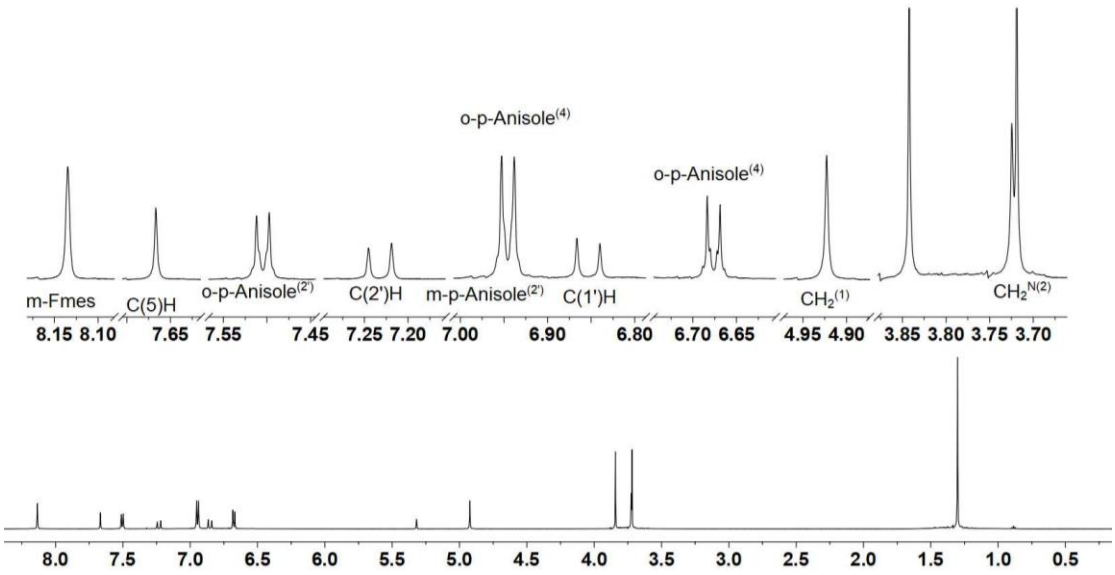


Figure S1. $^{1}$H NMR (600 MHz, methylene chloride-$d_2$, 299 K) spectrum of compound **4a**.

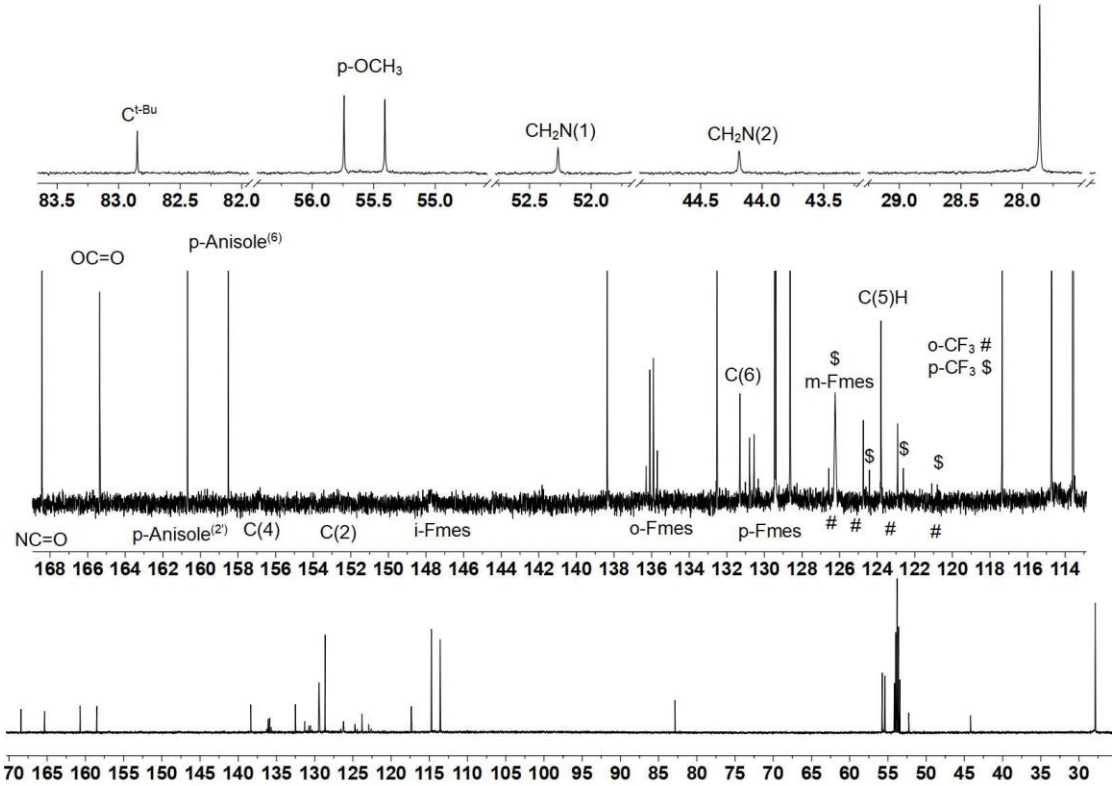


Figure S2. $^{13}$C{$^{1}$H} NMR (151 MHz, methylene chloride-$d_2$, 299 K) spectrum of compound **4a**.

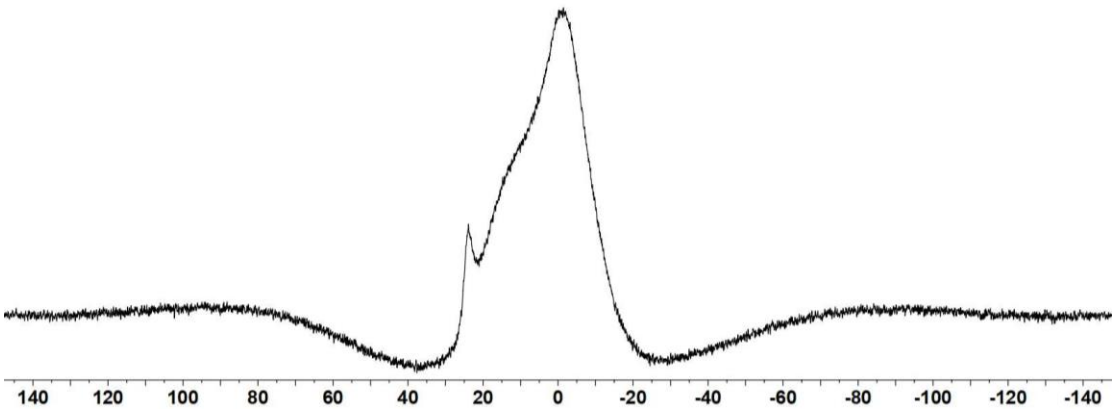

Figure S3. $^{11}B\{^{1}H\}$ NMR (192 MHz, methylene chloride-$d_2$, 299 K) spectrum of compound **4a**.

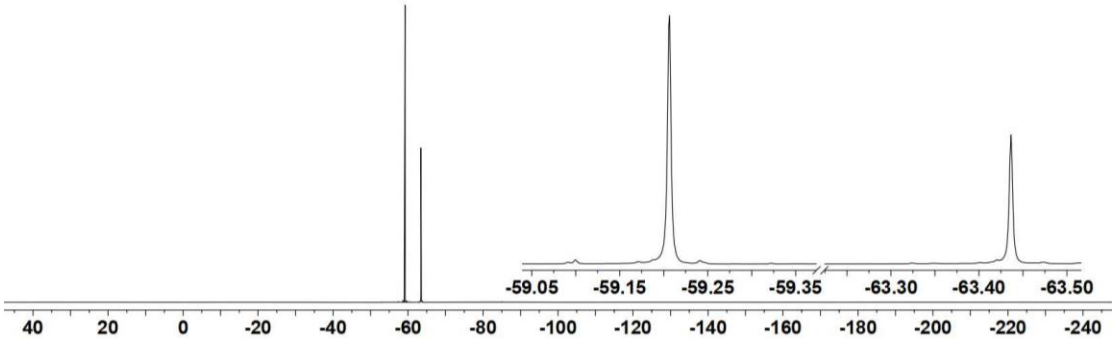

Figure S4. $^{19}F$ NMR (564 MHz, methylene chloride-$d_2$, 299 K) spectrum of compound **4a**.

Crystals of compound **4a** suitable for the X-ray crystal structure analysis were obtained from a solution of compound **4a** in a mixture of dichloromethane and n-pentane at-35 °C.

**X-ray crystal structure analysis of compound 4a (erk9839):** A yellow needle-like specimen of $C_{37.50}H_{33}BClF_9N_2O_5$, approximate dimensions 0.073 mm x 0.078 mm x 0.200 mm, was used for the X-ray crystallographic analysis. The X-ray intensity data were measured on a Bruker D8 Venture PHOTON III Diffractometer system equipped with a micro focus tube Cu Ims (CuKα, λ = 1.54178 Å) and a MX mirror monochromator. A total of 2253 frames were collected. The total exposure time was 23.14 hours. The frames were integrated with the Bruker SAINT software package using a wide-frame algorithm. The integration of the data using a triclinic unit cell yielded a total of 124898 reflections to a maximum θ angle of 68.42° (0.83 Å resolution), of which 13074 were independent (average redundancy 9.553, completeness = 97.3%, $R_{int}$ = 6.59%, $R_{sig}$ = 3.16%) and 10718 (81.98%) were greater than 2σ($F^2$). The final cell constants of a = 8.7527(2) Å, b = 21.1140(4) Å, c = 21.2756(4) Å, α = 105.5310(10)°, β = 100.8150(10)°, γ = 97.6900(10)°, volume = 3649.92(13) $Å^3$, are based upon the refinement of the XYZ-centroids of 9716 reflections above 20 σ(I) with 4.433° < 2θ < 136.3°. Data were corrected for absorption effects using the Multi-Scan method (SADABS). The ratio of minimum to maximum apparent transmission was 0.905. The calculated minimum and maximum transmission coefficients (based on crystal size) are 0.7200 and 0.8830. The structure was solved and refined using the Bruker SHELXTL Software Package, using the space group *P*-1, with Z = 4 for the formula unit, $C_{37.50}H_{33}BClF_9N_2O_5$. The final anisotropic full-matrix least-squares refinement on $F^2$ with 1010 variables converged at R1 = 3.45%, for the observed data and wR2 = 8.40% for all data. The goodness-of-fit was 1.031. The largest peak in the final difference electron

density synthesis was 0.352 $e^-/Å^3$ and the largest hole was -0.319 $e^-/Å^3$ with an RMS deviation of 0.045 $e^-/Å^3$. On the basis of the final model, the calculated density was 1.472 $g/cm^3$ and F(000), 1660 $e^-$. CCDC number: 2055393.

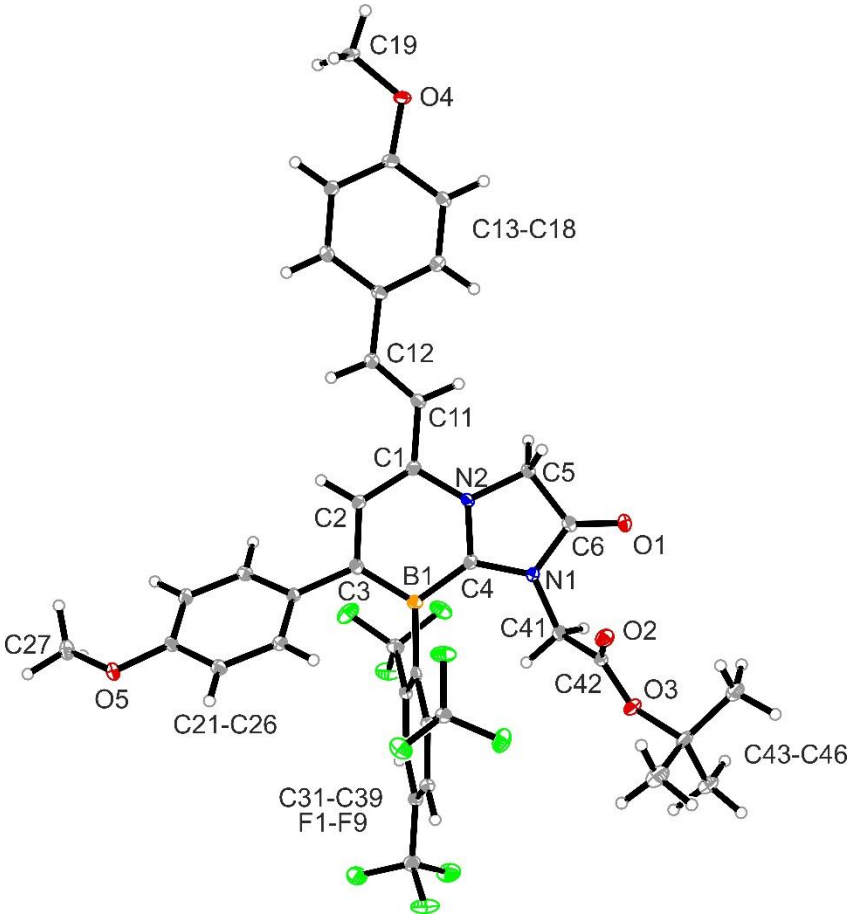


Figure S5. Crystal structure of compound **4a**. [Only one molecule (molecule "A") of two found in the asymmetric unit is shown. Thermal ellipsoids are set at 30% probability].

## Preparation of compound 4b

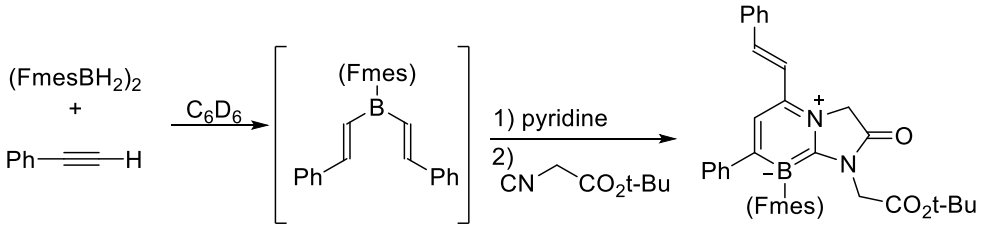


Scheme S2

At room temperature, phenylacetylene (40.8 mg, 0.4 mmol, 2 equiv.) was added to a suspension of borane **7** (58.8 mg, 0.1 mmol, 1 equiv.) in $C_6D_6$ (1 mL). The mixture was stirred at room temperature for 30 min to give a yellow solution. Pyridine (79 mg, 1 mmol, 5 equiv.) was added to the solution and stirred for 5 min. Then isocyanide **8** (56.4 mg, 0.4 mmol, 2 equiv.) in $C_6D_6$ (1 mL) was added to the solution. The mixture was stirred for 2 days. All volatiles were removed in vacuum.

The residue was purified via chromatography of silica gel with dichloromethane as eluents to give the compound **4b** as yellow solid (41 mg, 29 % yield).

**HRMS** for $C_{35}H_{28}BF_9N_2O_3^+$ ($M^+$): Calc. (706.2050), Found: 706.2057.

**$^1$H NMR** (600 MHz, methylene chloride-$d_2$, 299 K): δ = 8.13 (s, 2H, *m*-Fmes), 7.73 (s, 1H, C(5)H), 7.57 (m, 2H, *o*-$Ph^{(2')}$), 7.42 (m, 2H, *m*-$Ph^{(2')}$), 7.34 (m, 1H, *p*-$Ph^{(2')}$), 7.29 (d, $^3J_{HH}$ = 15.8 Hz, 1H, C(2')H), 7.15 (m, 2H, *m*-$Ph^{(4)}$), 7.11 (m, 1H, *p*-$Ph^{(4)}$), 7.04 (m, 2H, *o*-$Ph^{(4)}$), 7.01 (d, $^3J_{HH}$ = 15.8 Hz, 1H, C(1')H), 4.96 (s, 2H, $CH_2^{(1)}$), 3.75 (s, 2H, $CH_2^{N(2)}$), 1.31 (s, 9H, $CH_3^{t\text{-}Bu}$).

**$^{13}$C{$^1$H} NMR** (151 MHz, methylene chloride-$d_2$, 299 K): δ = 168.5 (NC=O), 165.3 (OC=O), 157.0 (br, C(4)), 153.5 (br, C(2)), 147.2 (br, *i*-Fmes), 145.9 (*i*-$Ph^{(4)}$), 136.7 (*i*-$Ph^{(2')}$), 136.0 (q, $^2J_{FC}$ = 29.7 Hz, *o*-Fmes), 132.8 (C(2)'H), 130.80 (q, $^2J_{FC}$ = 34.8 Hz, *p*-Fmes), 130.79 (C(6)), 129.3 (*m*-$Ph^{(2')}$), 129.1 (*p*-$Ph^{(2')}$), 128.4 (*o*-$Ph^{(4)}$), 128.2 (*m*-$Ph^{(4)}$), 127.3 (*o*-$Ph^{(2')}$), 126.3 (*p*-$Ph^{(4)}$), 126.2 (br m, *m*-Fmes), 124.6 (C(5)H), 123.8 (q, $^1J_{FC}$ = 275.0 Hz, *o*-$CF_3$), 123.5 (q, $^1J_{FC}$ = 273.0 Hz, *p*-$CF_3$), 119.5 (C(1')H), 83.0 ($C^{t\text{-}Bu}$), 52.3 ($CH_2^{(1)}$), 44.2 ($CH_2^{N(2)}$), 27.9 ($CH_3^{t\text{-}Bu}$).

**$^{11}$B{$^1$H} NMR** (192 MHz, methylene chloride-$d_2$, 299 K): δ = 24.6 ($v_{1/2}$ ≈ 500 Hz).

**$^{19}$F NMR** (564 MHz, methylene chloride-$d_2$, 299 K): δ = -59.1 (s, 2F, *o*-$CF_3$), -63.5 (s, 1F, *p*-$CF_3$).

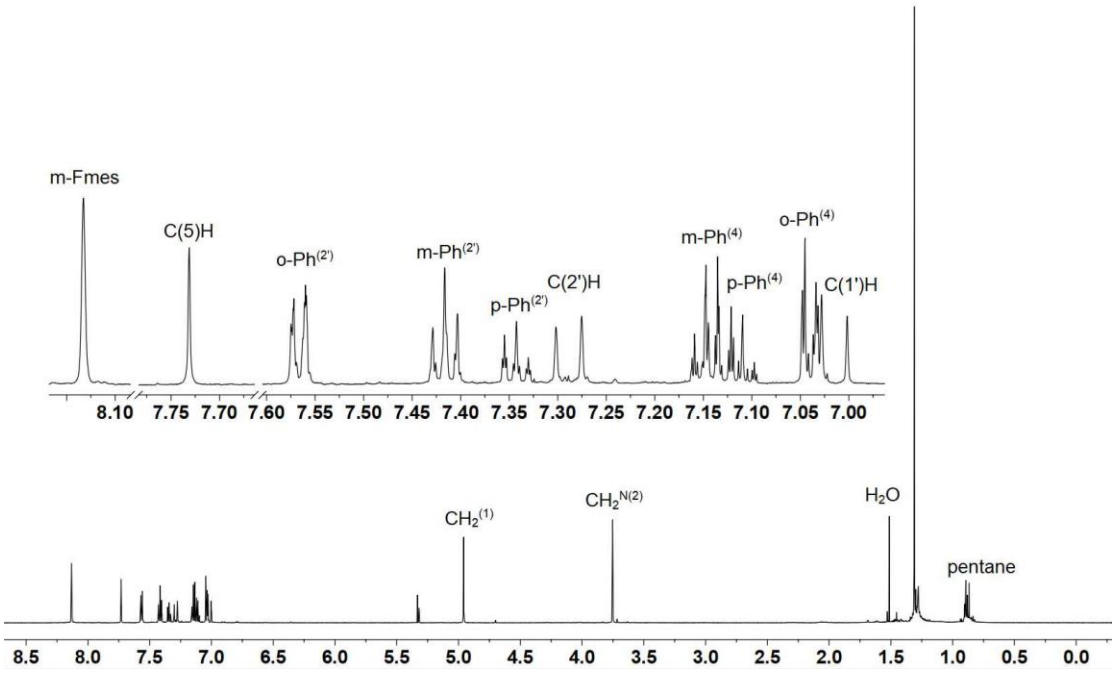


Figure S6. $^1$H NMR (600 MHz, methylene chloride-$d_2$, 299 K) spectrum of compound **4b**.

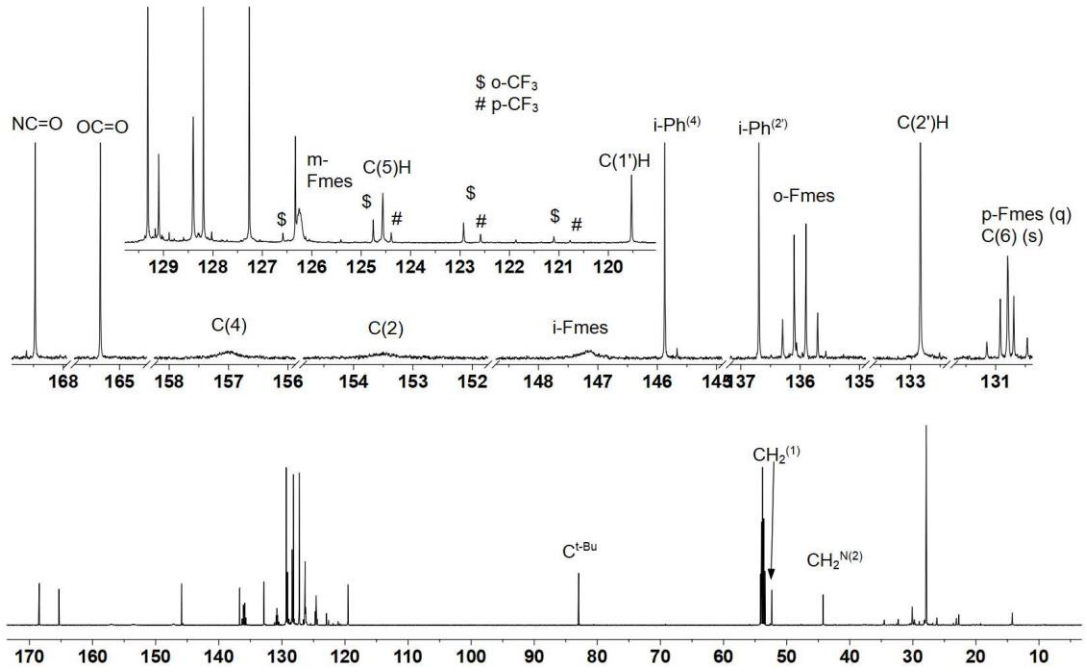


Figure S7. $^{13}C\{^{1}H\}$ NMR (151 MHz, methylene chloride-$d_2$, 299 K) spectrum of compound **4b.**

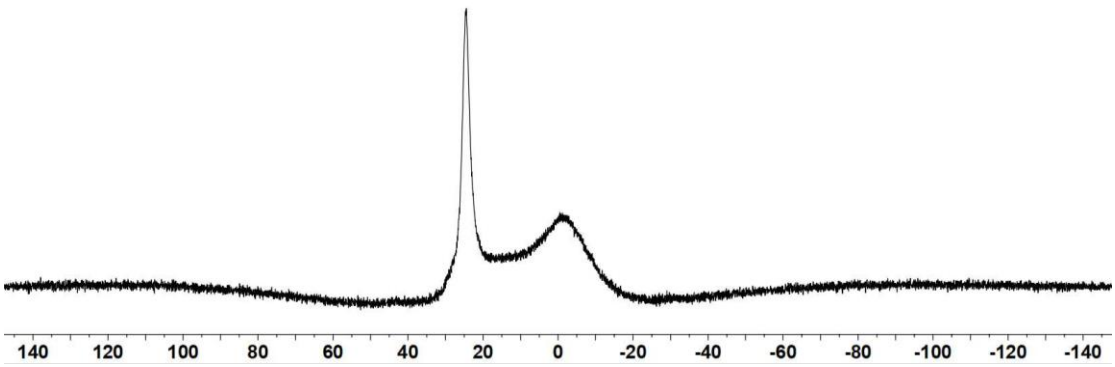

Figure S8. $^{11}B\{^{1}H\}$ NMR (192 MHz, methylene chloride-$d_2$, 299 K) spectrum of compound **4b**.

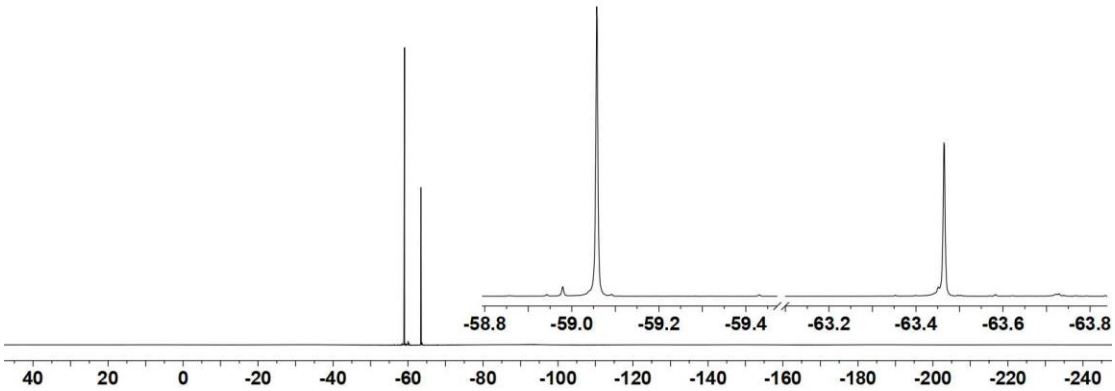

Figure S9. $^{19}F$ NMR (564 MHz, methylene chloride-$d_2$, 299 K) spectrum of compound **4b**.

Crystals of compound **4b** suitable for the X-ray crystal structure analysis were obtained from a solution of compound **4b** in cyclopentane at-35 °C.

**X-ray crystal structure analysis of compound 4b (erk9731):** A yellow needle-like specimen of $C_{35}H_{28}BF_9N_2O_3$, approximate dimensions 0.052 mm x 0.076 mm x 0.189 mm, was used for the X-ray crystallographic analysis. The X-ray intensity data were measured. A total of 1054 frames were collected. The total exposure time was 18.23 hours. The frames were integrated with the Bruker SAINT software package using a wide-frame algorithm. The integration of the data using a triclinic unit cell yielded a total of 51792 reflections to a maximum θ angle of 66.84° (0.84 Å resolution), of which 11739 were independent (average redundancy 4.412, completeness = 99.5%, $R_{int}$ = 6.47%, $R_{sig}$ = 5.11%) and 8503 (72.43%) were greater than $2\sigma(F^2)$. The final cell constants of a = 13.6617(3) Å, b = 14.0040(3) Å, c = 18.5575(4) Å, α = 70.2330(10)°, β = 87.7710(10)°, γ = 83.5410(10)°, volume = 3319.98(13) $Å^3$, are based upon the refinement of the XYZ-centroids of 9941 reflections above 20 σ(I) with 5.06° < 2θ < 133.5°. Data were corrected for absorption effects using the multi-scan method (SADABS). The ratio of minimum to maximum apparent transmission was 0.882. The calculated minimum and maximum transmission coefficients (based on crystal size) are 0.8220 and 0.9460. The structure was solved and refined using the Bruker SHELXTL Software Package, using the space group *P*-1, with Z = 4 for the formula unit, $C_{35}H_{28}BF_9N_2O_3$. The final anisotropic full-matrix least-squares refinement on $F^2$ with 1000 variables converged at R1 = 5.27%, for the observed data and wR2 = 14.82% for all data. The goodness-of-fit was 1.020. The largest peak in the final difference electron density synthesis was 0.718 $e^-/Å^3$ and the largest hole was -0.272 $e^-/Å^3$ with an RMS deviation of 0.056 $e^-/Å^3$. On the basis of the final model, the calculated density was 1.413 $g/cm^3$ and F(000), 1448 $e^-$. CCDC number: 2055394.

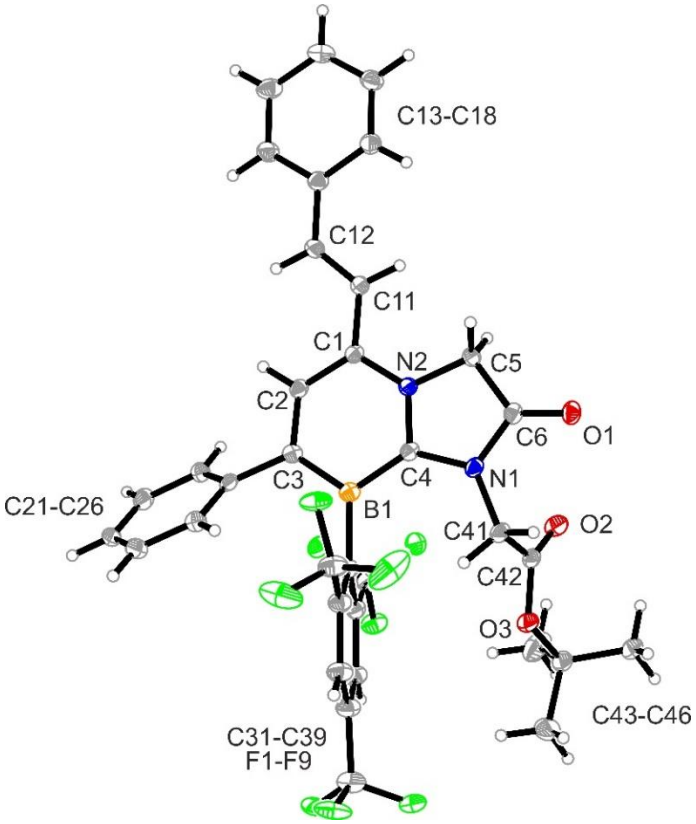


Figure S10. Crystal structure of compound **4b**. (Only one molecule (molecule "A") of two found in the asymmetric unit is shown. Thermal ellipsoids are set at 30% probability.)

## Preparation of compound 4c

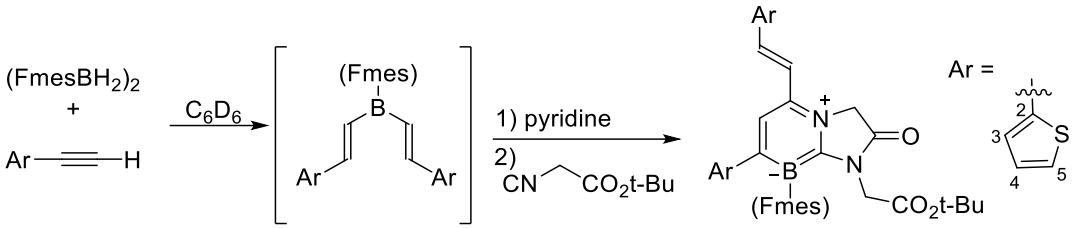


Scheme S3.

At room temperature, 2-ethynylthiophene (43.2 mg, 0.4 mmol, 2 equiv.) was added to a suspension of borane **7** (58.8 mg, 0.1 mmol, 1 equiv.) in $C_6D_6$ (1 mL). The mixture was stirred at room temperature for 30 min to give a yellow solution. Pyridine (79 mg, 1 mmol, 5 equiv.) was added to the solution and stirred for 5 min. Then isocyanide **8** (56.4 mg, 0.4 mmol, 2 equiv.) in $C_6D_6$ (1 mL) was added to the solution. The mixture was stirred for 2 days. All volatiles were removed in vacuum. The residue was purified via chromatography of silica gel with dichloromethane as eluents to give the compound **4c** as yellow solid (39 mg, 27 % yield).

**HRMS** for $C_{31}H_{24}BF_9N_2O_3S_2^+$ ($M^+$): Calc. (718.1178), Found: 718.1181.

[thio: thiophen-2-yl]

**$^1$H NMR** (600 MHz, methylene chloride-$d_2$, 299 K): δ = 8.22 (s, 2H, *m*-Fmes), 7.86 (s, 1H, C(5)H), 7.42 (d, $^3J_{HH}$ = 15.6 Hz, 1H, C(2')H), 7.34 (d, $^3J_{HH}$ = 5.1 Hz, 1H, C(5)H$^{thio(2')}$), 7.22 (d, $^3J_{HH}$ = 3.5 Hz, 1H, C(3)H$^{thio(2')}$), 7.13 (dd, $^3J_{HH}$ = 5.1 Hz, $^4J_{HH}$ = 1.1 Hz, 1H, C(5)H$^{thio(4)}$), 7.08 (dd, $^3J_{HH}$ = 5.1, 3.5 Hz, 1H, C(4)H$^{thio(2')}$), 6.84 (dd, $^3J_{HH}$ = 5.1, 3.7 Hz, 1H, C(4)H$^{thio(4)}$), 6.78 (d, $^3J_{HH}$ = 15.6 Hz, 1H, C(1')H), 6.63 (dd, $^3J_{HH}$ = 3.7 Hz, $^4J_{HH}$ = 1.1 Hz, 1H, C(3)H$^{thio(4)}$), 4.89 (s, 2H, $CH_2^{(1)}$), 3.72 (s, 2H, $CH_2^{N(2)}$), 1.31 (s, 9H, $CH_3^{t\text{-}Bu}$).

**$^{13}$C{$^1$H} NMR** (151 MHz, methylene chloride-$d_2$, 299 K) [selected resonances]: δ = 168.3 (NC=O), 165.2 (OC=O), 154.3 (br, C(2)), 148.8 (C(2)$^{thio(4)}$), 147.4 (br, C(4)), 147.2 (*i*-Fmes), 141.9 (C(2)$^{thio(2')}$), 136.3 (q, $^2J_{FC}$ = 29.9 Hz, *o*-Fmes), 131.3 (q, q = 34.5 Hz, *p*-Fmes), 130.6 (C(6)), [128.48, 128.47] (C(3,4)H$^{thio(2')}$), 127.6 (C(4)H$^{thio(4)}$), 126.5 (*m*-Fmes, C(5)$^{thio(2')}$), 126.0 (C(2')H), 125.6 (C(5)H$^{thio(4)}$), 125.0 (C(3)H$^{thio(4)}$), 123. 8 (q, $^1J_{FC}$ = 275.3 Hz, *o*-$CF_3$), 123. 5 (q, $^1J_{FC}$ = 271.4 Hz, *p*-$CF_3$), 121.9 (C(5)H), 118.6 (C(1')H), 82.9 ($C^{t\text{-}Bu}$), 52.2 ($CH_2^{(1)}$), 44.2 ($CH_2^{N(2)}$), 27.9 ($CH_3^{t\text{-}Bu}$).

**$^{11}$B{$^1$H} NMR** (192 MHz, methylene chloride-$d_2$, 299 K): δ = 24.2 ($v_{1/2}$ ≈ 400 Hz).

**$^{19}$F NMR** (564 MHz, methylene chloride-$d_2$, 299 K): δ = -59.9 (s, 2F, *o*-$CF_3$), -63.4 (s, 1F, *p*-$CF_3$).

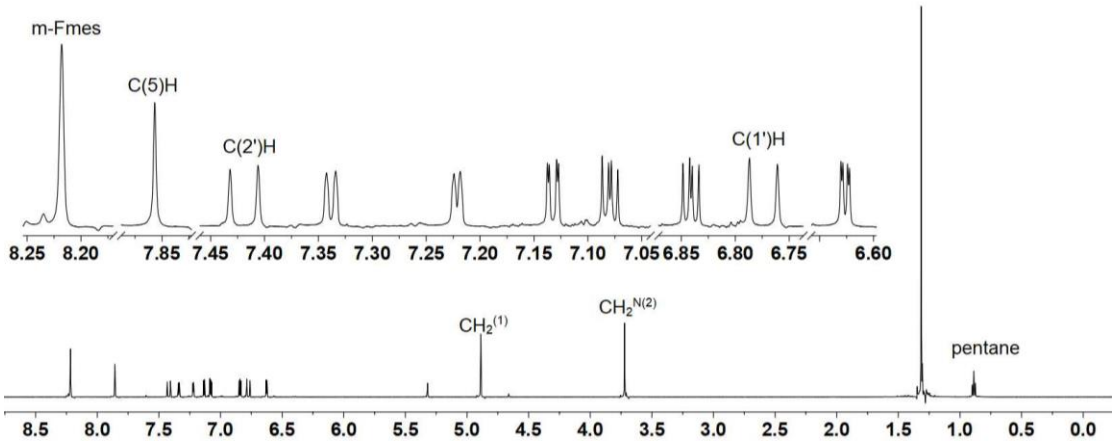


Figure S11. $^{1}$H NMR (600 MHz, methylene chloride-$d_2$, 299 K) spectrum of compound **4c**.

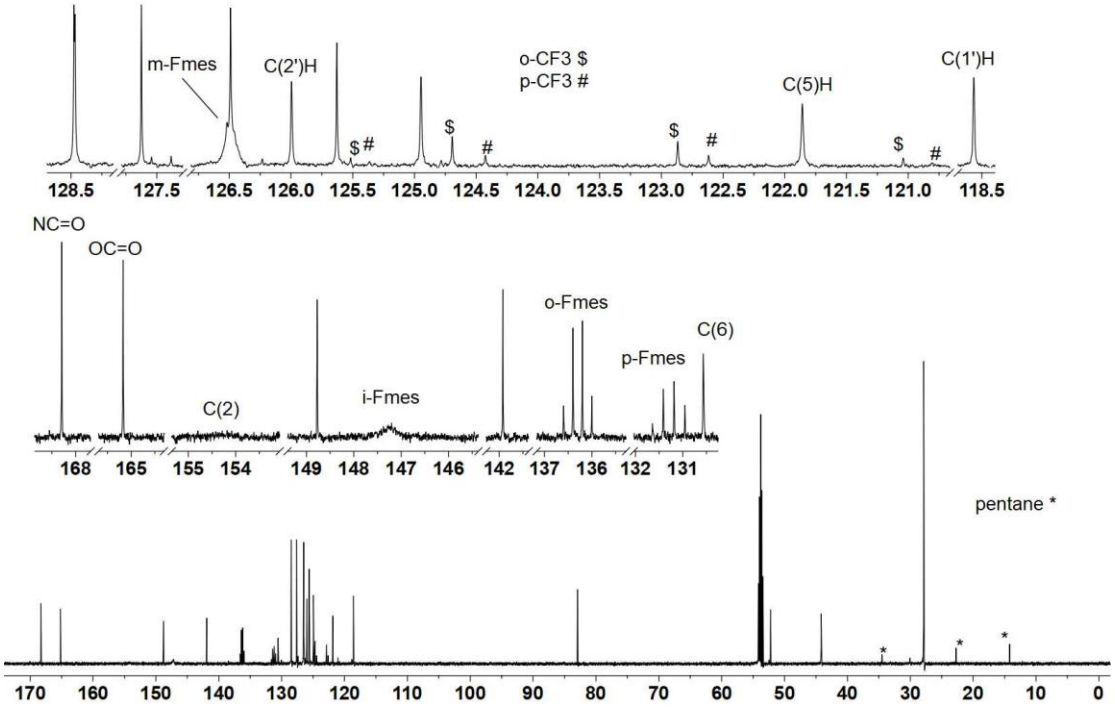


Figure S12. $^{13}$C{$^{1}$H} NMR (151 MHz, methylene chloride-$d_2$, 299 K) spectrum of compound **4c**.

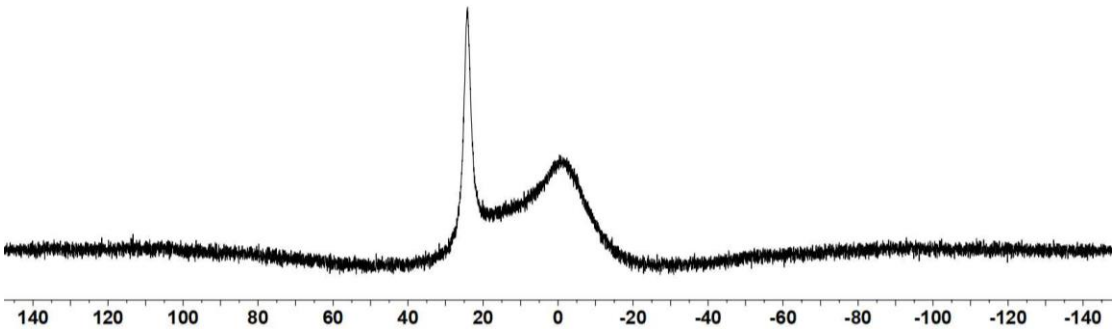

Figure S13. $^{11}$B{$^{1}$H} NMR (192 MHz, methylene chloride-$d_2$, 299 K) spectrum of compound **4c**.

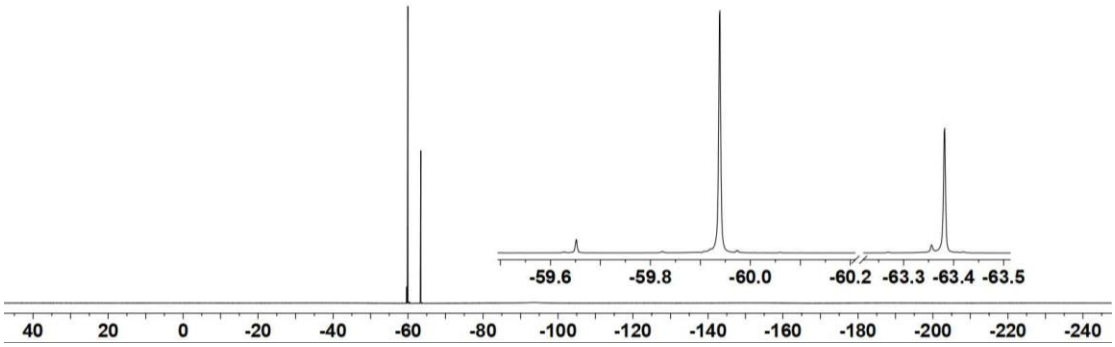


Figure S14. $^{19}F$ NMR (564 MHz, methylene chloride-$d_2$, 299 K) spectrum of compound **4c**.

Crystals of compound **4c** suitable for the X-ray crystal structure analysis were obtained from a solution of compound **4c** in dichloromethane and n-heptane at room temperature.

**X-ray crystal structure analysis of compound 4c (erk9828):** A yellow prism-like specimen of $C_{31}H_{24}BF_9N_2O_3S_2$, approximate dimensions 0.109 mm x 0.135 mm x 0.177 mm, was used for the X-ray crystallographic analysis. The X-ray intensity data were measured on a Bruker D8 Venture PHOTON III Diffractometer system equipped with a micro focus tube Cu Ims (CuKα, λ = 1.54178 Å) and a MX mirror monochromator. A total of 1214 frames were collected. The total exposure time was 15.79 hours. The frames were integrated with the Bruker SAINT software package using a wide-frame algorithm. The integration of the data using a monoclinic unit cell yielded a total of 103772 reflections to a maximum θ angle of 66.67° (0.84 Å resolution), of which 10737 were independent (average redundancy 9.665, completeness = 97.4%, $R_{int}$ = 8.54%, $R_{sig}$ = 3.75%) and 8381 (78.06%) were greater than $2\sigma(F^2)$. The final cell constants of a = 15.1630(3) Å, b = 26.2070(5) Å, c = 15.9881(3) Å, β = 101.0680(10)°, volume = 6235.1(2) $Å^3$, are based upon the refinement of the XYZ-centroids of 9866 reflections above 20 σ(I) with 5.939° < 2θ < 132.8°. Data were corrected for absorption effects using the Multi-Scan method (SADABS). The ratio of minimum to maximum apparent transmission was 0.909. The calculated minimum and maximum transmission coefficients (based on crystal size) are 0.6780 and 0.7820. The structure was solved and refined using the Bruker SHELXTL Software Package, using the space group $P2_1/c$, with Z = 8 for the formula unit, $C_{31}H_{24}BF_9N_2O_3S_2$. The final anisotropic full-matrix least-squares refinement on $F^2$ with 1001 variables converged at R1 = 4.13%, for the observed data and wR2 = 11.03% for all data. The goodness-of-fit was 1.012. The largest peak in the final difference electron density synthesis was 0.466 $e^-/Å^3$ and the largest hole was -0.556 $e^-/Å^3$ with an RMS deviation of 0.052 $e^-/Å^3$. On the basis of the final model, the calculated density was 1.531 $g/cm^3$ and F(000), 2928 $e^-$. CCDC number: 2055395.

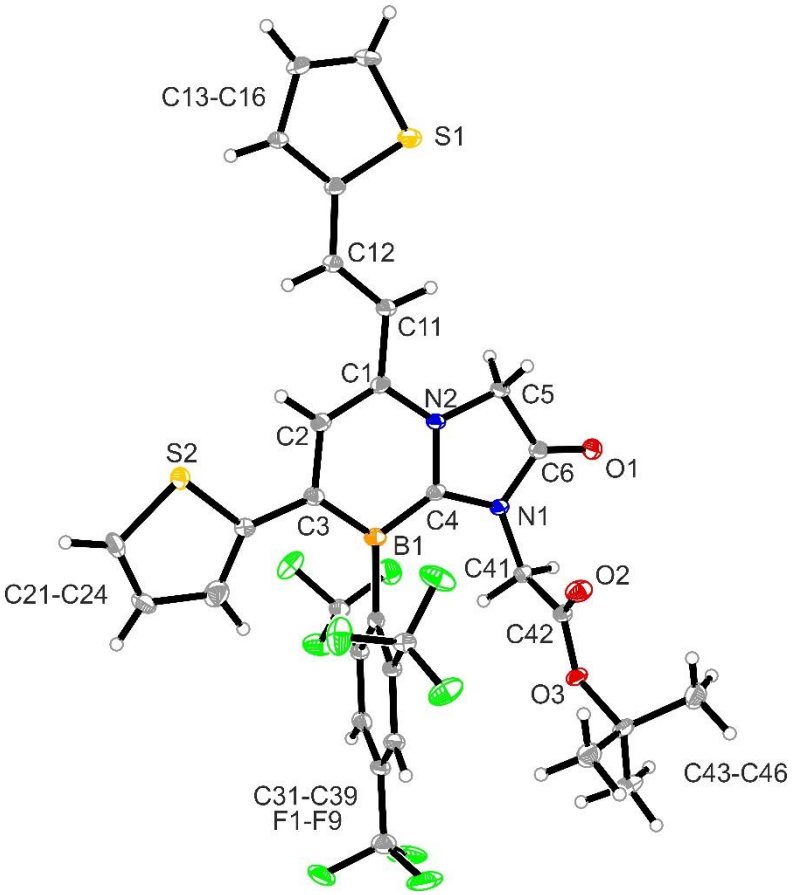


Figure S15. Crystal structure of compound **4c**. (Only one molecule (molecule "A") of two found in the asymmetric unit is shown. Thermal ellipsoids are set at 30% probability.)

## Preparation of compound 4d

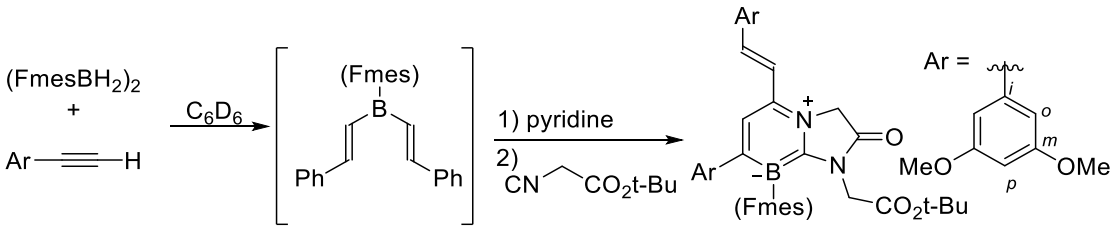


Scheme S4.

At room temperature, phenylacetylene (64.8 mg, 0.4 mmol, 2 equiv.) was added to a suspension of borane **7** (58.8 mg, 0.1 mmol, 1 equiv.) in $C_6D_6$ (1 mL). The mixture was stirred at room temperature for 30 min to give a yellow solution. Pyridine (79 mg, 1 mmol, 5 equiv.) was added to the solution and stirred for 5 min. Then isocyanide **8** (56.4 mg, 0.4 mmol, 2 equiv.) in $C_6D_6$ (1 mL) was added to the solution. The mixture was stirred for 2 days. All volatiles were removed in vacuum. The residues were purified via chromatography of silica gel with pentane: ethyl acetate = 4: 1 as eluents to give the compound **4d** as yellow solid (60 mg, 36 % yield).

**HRMS** for $C_{39}H_{36}BF_9N_2O_7Na^+$ ([M + Na]$^+$): Calc. (849.2371), Found: (849.2374).

[Ar: 3,5-dimethoxy phenyl]

**$^{1}$H NMR** (600 MHz, methylene chloride-$d_2$, 299 K): δ = 8.14 (s, 2H, *m*-Fmes), 7.74 (s, 1H, C(5)H), 7.21 (d, $^{3}J_{HH}$ = 15.8 Hz, 1H, C(2')H), 6.98 (d, $^{3}J_{HH}$ = 15.8 Hz, 1H, C(1')H), 6.70 (d, $^{4}J_{HH}$ = 2.2 Hz, 2H, *o*-$Ar^{(2')}$), 6.46 (t, $^{4}J_{HH}$ = 2.2 Hz, 1H, *p*-$Ar^{(2')}$), 6.22 (t, $^{4}J_{HH}$ = 2.3 Hz, 1H, *p*-$Ar^{(4)}$), 6.18 (d, $^{4}J_{HH}$ = 2.3 Hz, 2H, *o*-$Ar^{(4)}$), 4.97 (s, 2H, $CH_2^{(1)}$), 3.84 (s, 6H, $OCH_3^{Ar(2')}$), 3.75 (s, 2H, $CH_2^{N(2)}$), 3.54 (s, 6H, $OCH_3^{Ar(4)}$), 1.31 (s, 9H, $CH_3^{t\text{-}Bu}$).

**$^{13}$C{$^{1}$H} NMR** (151 MHz, methylene chloride-$d_2$, 299 K): δ = 168.4 (NC=O), 165.3 (OC=O), 161.6 (*m*-$Ar^{(2')}$), 160.7 (*m*-$Ar^{(4)}$), 156.5 (br, C(4)), 153.8 (br, C(2)), 147.9 (*i*-$Ar^{(4)}$), 147.3 (br, *i*-Fmes), 138.5 (*i*-$Ar^{(2')}$), 136.0 (q, $^{2}J_{FC}$ = 29.7 Hz, *o*-Fmes), 132.9 (C(2)'H), 130.9 (q, $^{2}J_{FC}$ = 34.1 Hz, *p*-Fmes), 130.5 (C(6)), 126.3 (br m, *m*-Fmes), 124.4 (C(5)H), 123.8 (q, $^{1}J_{FC}$ = 275.8 Hz, *o*-$CF_3$), 123.5 (q, $^{1}J_{FC}$ = 273.0 Hz, *p*-$CF_3$), 119.9 (C(1')H), 106.5 (*o*-$Ar^{(4)}$), 105.3 (*o*-$Ar^{(2')}$), 101.2 (*p*-$Ar^{(2')}$), 98.9 (*p*-$Ar^{(4)}$), 83.0 ($C^{t\text{-}Bu}$), 55.8 ($OCH_3^{Ar(2')}$), 55.4 ($OCH_3^{Ar(4)}$), 52.4 ($CH_2^{(1)}$), 44.3 ($CH_2^{N(2)}$), 27.9 ($CH_3^{t\text{-}Bu}$).

**$^{11}$B{$^{1}$H} NMR** (192 MHz, methylene chloride-$d_2$, 299 K): δ = 24.4 ($v_{1/2}$ ≈ 460 Hz).

**$^{19}$F NMR** (564 MHz, methylene chloride-$d_2$, 299 K): δ = -59.0 (s, 2F, *o*-$CF_3$), -63.5 (s, 1F, *p*-$CF_3$).

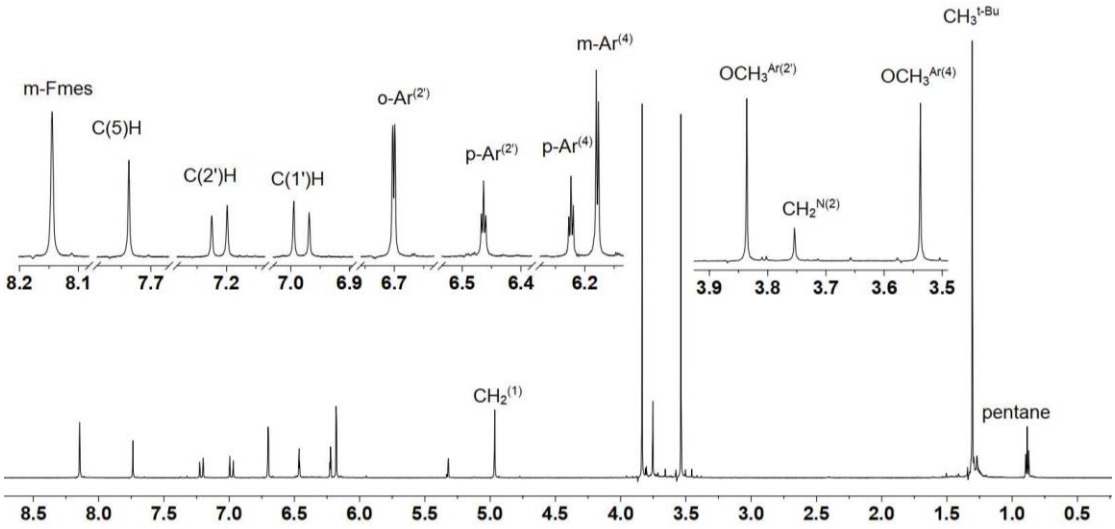


Figure S16. $^{1}$H NMR (600 MHz, methylene chloride-$d_2$, 299 K) spectrum of compound **4d**

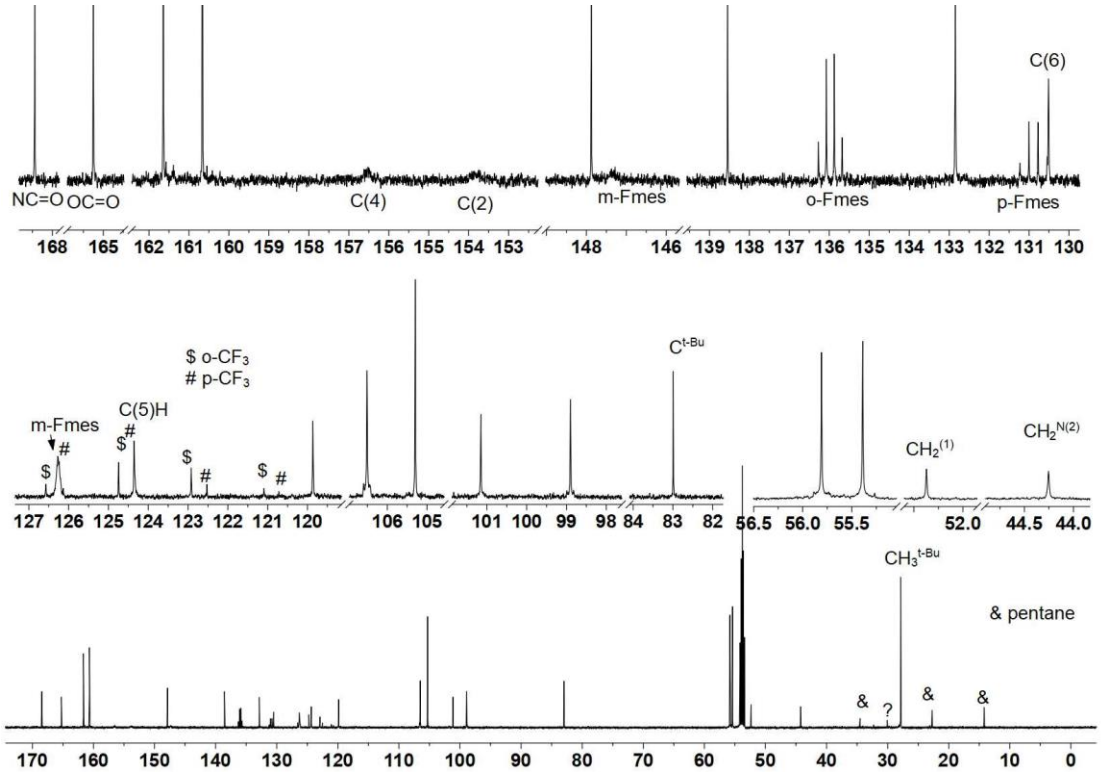


Figure S17. $^{13}C\{^{1}H\}$ NMR (151 MHz, methylene chloride-$d_2$, 299 K) spectrum of compound **4d**

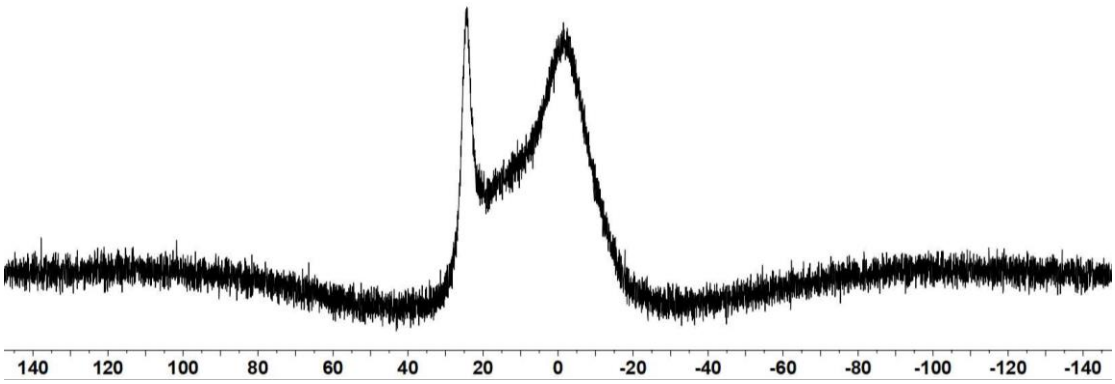

Figure S18. $^{11}B\{^{1}H\}$ NMR (192 MHz, methylene chloride-$d_2$, 299 K) spectrum of compound **4d**

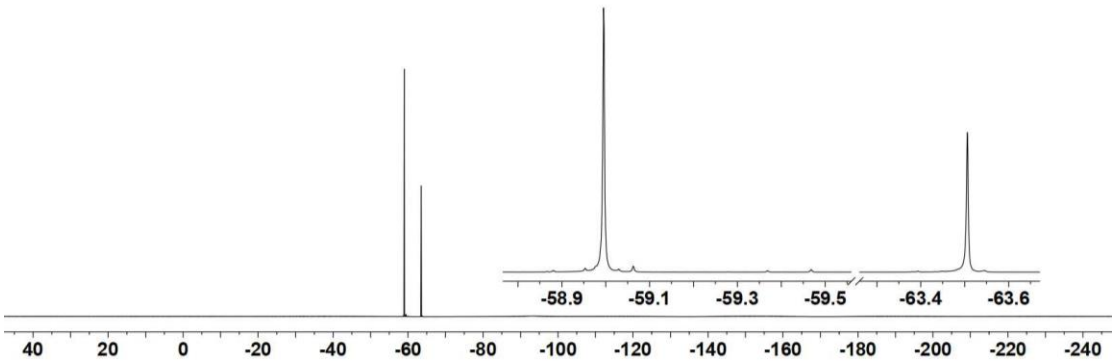

Figure S19. $^{19}F$ NMR (564 MHz, methylene chloride-$d_2$, 299 K) spectrum of compound **4d**.

## Photophysical properties

### General Procedures

The photophysical properties of all compounds were investigated by means of absorption and emission spectroscopy at micromolar concentrations. Initially, a stock solution of the respective compound was prepared in $CHCl_3$ (c = 1mM), of which aliquots were distributed into vials, and subsequently dried under an Argon stream. The dry residues were freshly dissolved in the appropriate amount of solvent to yield solutions with the desired concentration (generally c = 10 µM). The freshly prepared solutions were measured directly in order to prevent decomposition. For all preparation purposes and measurements, spectroscopic grade solvents were used.

#### UV-Vis absorption spectroscopy

UV-Vis absorption spectra were recorded on a JASCO V-750 with a spectral bandwidth of 1.0 nm and a scan rate of 1000 nm $min^{-1}$. Glass cuvettes with a path length of 1 cm were used.

### Fluorescence emission and excitation spectroscopy

Fluorescence emission and excitation spectra were recorded on a JASCO Spectrofluorometer FP-8500 in quartz cuvettes with a path length of 1 cm and an emission slit width of 5 nm. The relative quantum yields ($\Phi_F$) were measured at 20 °C at an excitation wavelength of $\lambda_{exc}$ = 350 nm, without degassing the solutions prior to the measurements. The absorbance intensities were kept below 0.1 in order to minimize re-absorption effects. The quantum yields were calculated with reference to quinine sulfate in 0.5 M $H_2SO_4$ as standard (refractive index $\eta_R = 1.346$, $\Phi_R = 0.546$)[5] by measuring the absorbance at 350 nm and the area under the emission peak (365 – 695 nm), according to the following equation:

$$\Phi_F = \Phi_R \left(\frac{A}{A_R}\right)\left(\frac{Abs_R}{Abs}\right)\left(\frac{\eta}{\eta_R}\right)^2$$

$\Phi_R$ – quantum yield of reference
$A$ – area under emission peak of sample
$A_R$ – area under emission peak of reference
$Abs_R$ – absorbance of reference at excitation wavelength
$Abs$ – absorbance of sample at excitation wavelength
$\eta$ – refractive index of sample
$\eta_R$ – refractive index of reference

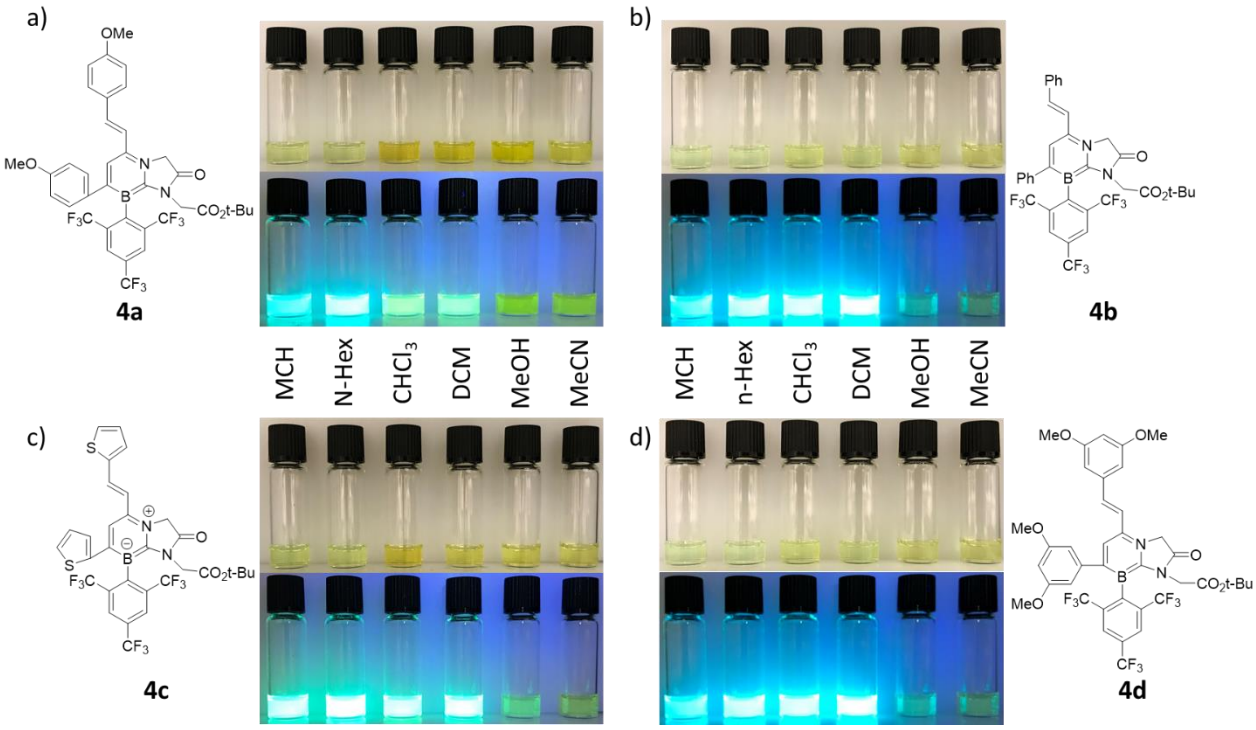


Figure S20. Photographs of solutions of the four investigated 1,3-BN-oxindole derivatives in different solvents, taken under ambient light (top panel) and under UV-irradiation at $\lambda_{exc.}$ = 365 nm (bottom panel, c = 10 µM, T = 293 K).

**Absorption properties**

Absorption spectra were recorded in solvents of different polarity (methylcyclohexane, *n*-hexane, DCM, chloroform, MeOH, MeCN) at a concentration of *c* = 10 µM (Figure S2). Despite the broad polarity range, all compounds were soluble in all investigated solvents. All of the compounds exhibit two primary absorption bands centred in the region between 300-350 nm and 400-450 nm, arising from $\pi \rightarrow \pi^*$ transitions of the aromatic 1,3-BN-oxindole moiety. Variation of the solvent has only a minimal effect on the location of these maxima ($\Delta\lambda \sim 10$ nm), indicating a negligible effect of solvent polarity on the relative stability of the corresponding ground and excited states (solvatochromic effect). Molecules **4b** (phenyl-) and **4d** (3,5-dimethoxyphenyl-) both show equal properties in all solvents, whereas the more electron rich derivatives **4a** (*p*-anisyl-) and **4c** (thienyl-) exhibit slightly different spectra. The spectra of these electron-rich derivatives show an absorption shoulder in the low-energy region ($\lambda \sim 500$ nm), whose intensity is affected by the solvent polarity. In apolar solvents (*n*-Hex, MCH) this shoulder vanishes, whereas in more polar solvents (DCM, $CHCl_3$, MeOH, MeCN), it is present. The low energy and low intensity of this band points to a charge-transfer transition. This is supported by the fact that the absorption band is more pronounced in polar solvents. In charge-transfer transitions, the excited state is more polar due to the charge-separation upon excitation. Thus, the excited state is superiorly stabilized in more polar media. Considering the molecular structure of the investigated compounds, the charge-transfer could occur between the electron-rich 1,3-BN-oxindole moiety and the electron-poor Fmes-group. The substitution of the 1,3-BN-oxindole core considerably impacts the charge-transfer: derivatives **4c** (thienyl-) and **4a** (p-anisyl) strongly increase the electron density in the donating moiety, resulting in the appearance of the charge-transfer band. Derivatives **4b** (phenyl-) and **4d** (3,5-dimethoxyphenyl) on the other hand, lack the ability to significantly increase the electron density in the aromatic B,N-2-oxaindoline moiety, resulting in the absence of a charge-transfer band.

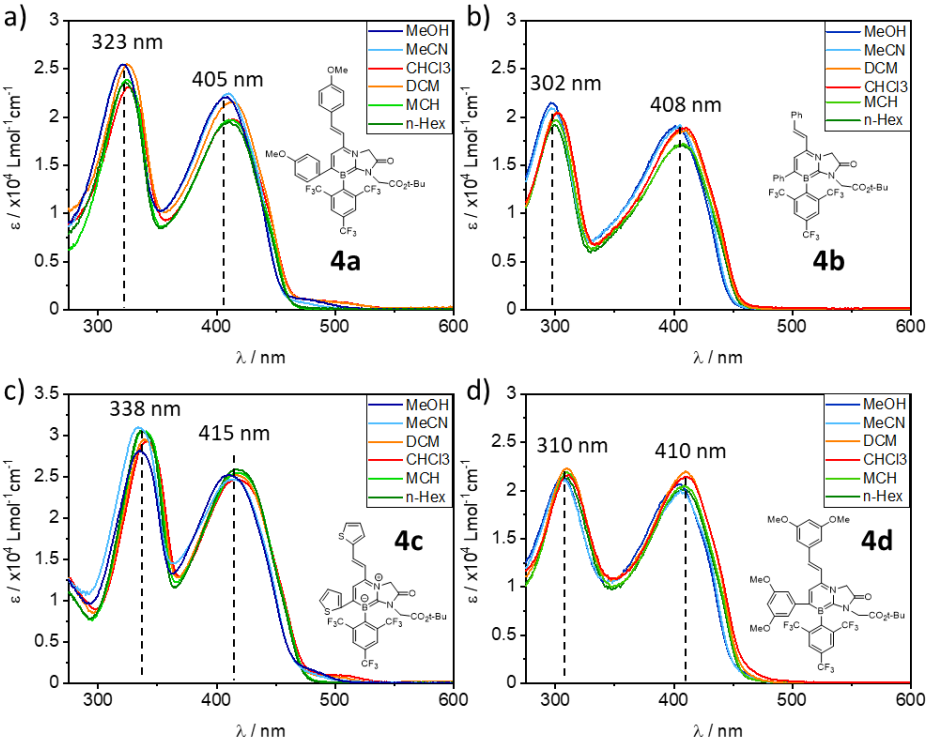


Figure S21. Absorption spectra of the four investigated 1,3-BN-oxindole derivatives in different solvents (*c* = 10 µM, *T* = 298 K).

**Fluorescence emission spectra**

Parallel to the absorption measurements, emission studies were carried out, exciting the molecules at the wavelengths of the respective absorption maxima. For all derivatives, excitation at both absorption maxima (~300-350 nm and ~400-450 nm) resulted in equal emission spectra, albeit the intensities varied. Figure S22 shows the emission spectra upon excitation of the transition around 405 nm. The emission shows a vibronic pattern with two maxima, whose wavelength slightly differs for the four derivatives. As the fluorescence emission always takes place from the vibronic ground state ($\nu_0$) of the first excited state ($S_1$), the two absorption bands must belong to the same electronic transition into different excited states. Thus, the high energy band is assigned to the $S_0 \rightarrow S_2$ transition and the band between ~400-450 nm is assigned to the corresponding $S_0 \rightarrow S_1$ transition. Excitation at 500 nm, where the charge-transfer band appears, resulted in spectra with very low emission intensities ($\lambda_{max}$ ~ 543 nm), which matches well with a charge transfer-nature of this absorption band.

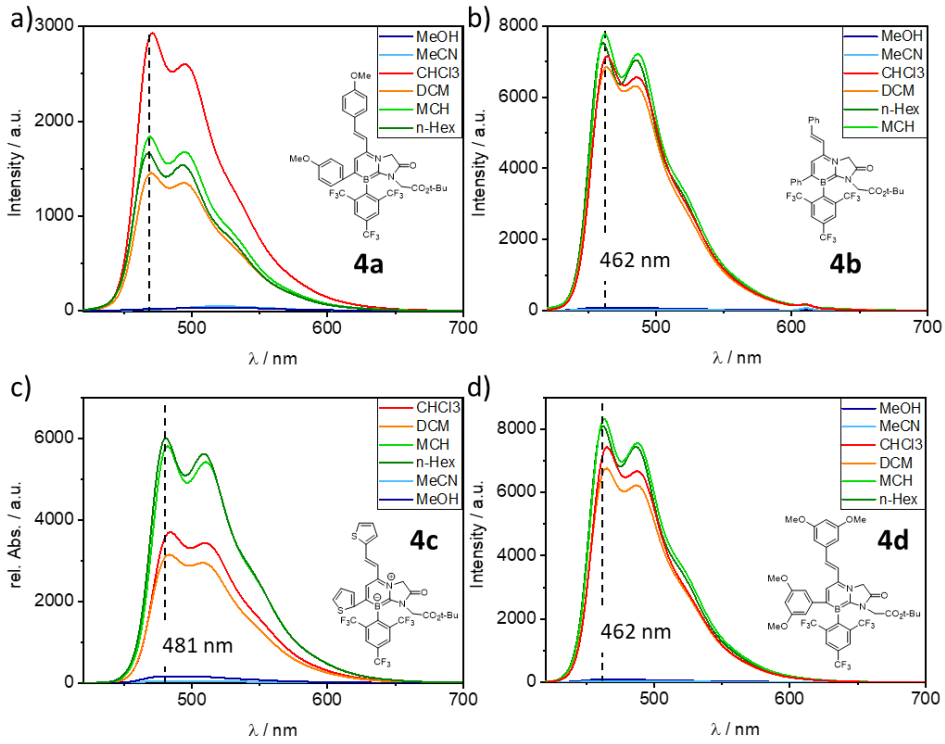


Figure S22. Fluorescence emission spectra of the four investigated 1,3-BN-oxindole derivatives in different solvents (c = 10 µM, T = 298 K, $\lambda_{exc}$ = 405 nm).

**Fluorescence Excitation spectra**

By registering excitation spectra, the transition assignments of the absorption bands could be confirmed. Monitoring the wavelength of maximum emission of each molecule resulted in excitation spectra which exbibit the same two, intense bands as the absorption spectra (Figure S23). This supports the $S_0 \rightarrow S_1$ and $S_0 \rightarrow S_2$ assignment of the $\pi \rightarrow \pi^*$ transition. Due to the very low intensity emission of the charge-transfer excited state, the excitation at its emission wavelength (543 nm) was recorded only in MeOH and MeCN, where the contamination of fluorescence emission from the $\pi \rightarrow \pi^*$ transition is the lowest. In Figure S23a and S24c, these excitation spectra are compared to the excitation spectra of the $\pi \rightarrow \pi^*$ transition for compounds **4a** and **4c**. Clearly, the excitation spectra are different, with new excitation bands in the region between 450 nm to above 500 nm (blue and cyan spectra). This substantiates that the high-wavelength absorption shoulder originates from a different electronic transition, namely the charge-transfer.

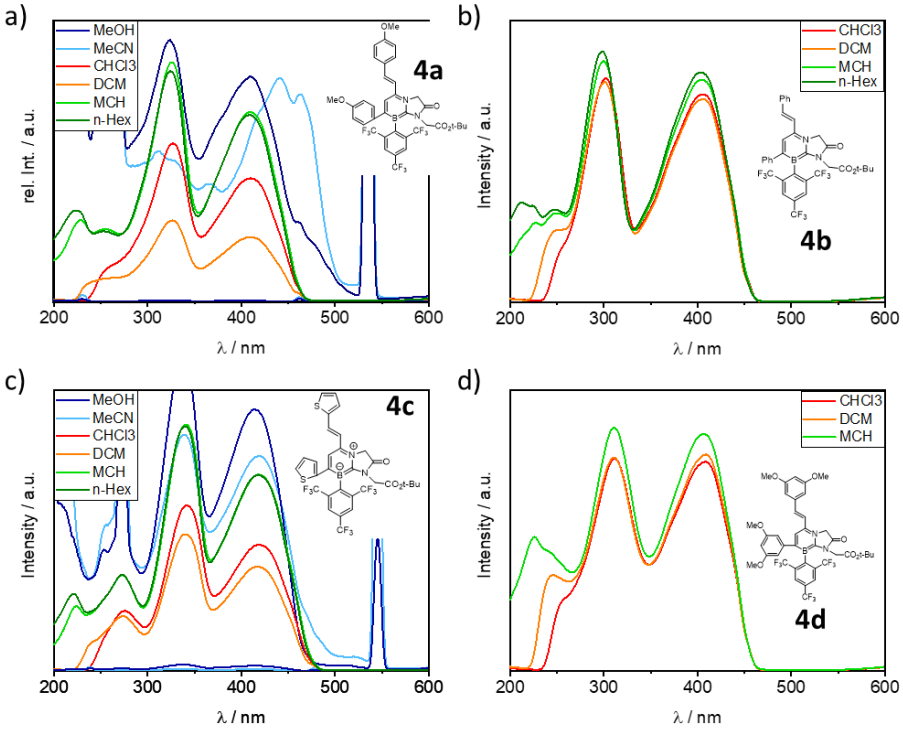


Figure S23. Fluorescence excitation spectra of the four investigated 1,3-BN-oxindole derivatives in different solvents. The spectra measured in $CHCl_3$, DCM, MCH and *n*-Hex were recorded at an emission wavelength of $\lambda_{em.}$ = 469 nm, whereas the spectra measured in MeOH and MeCN were obtained at an emission wavelength of $\lambda_{em.}$ = 543 nm.

## Fluorescence quantum yields

Remarkably, the fluorescence of all compounds was drastically quenched in the most polar solvents, which can even be observed with the bare eye (see photographs in Figure S20**Fehler! Verweisquelle konnte nicht gefunden werden.**). To quantitatively assess this effect, the relative fluorescence quantum yields of the compounds were registered in the six solvents (Table S1). All of the compounds display quantum yields of around 40-50 % in the most apolar solvents (color code green). From the obtained data, three important observations are made: A) The overall quantum yields of the compounds exhibiting the charge-transfer band are lower than those of the derivatives lacking the charge-transfer. B) The quantum yields of the compounds which do not exhibit charge-transfer behavior are similar in apolar solvents (MCH, *n*-Hex) and solvents of intermediate polarity ($CHCl_3$, DCM). For the derivatives exhibiting charge-transfer, in contrast, the quantum yields are 10-20 % higher in the apolar solvents (color code green *vs.* orange). C) The quantum yield of all compounds is below 1 % in the most polar solvents (MeOH, MeCN, color code red).

**Table S1**. Relative fluorescence quantum yields of the four investigated 1,3-BN-oxindole derivatives in different solvents.

| | QY CHCl3 | QY DCM | QY MCH | QY n-Hex | QY MeOH | QY MeCN |
|---|---|---|---|---|---|---|
| **4a** | 36.1 | 20.1 | 45.8 | 42.1 | 0.4 | 0.3 |
| **4b** | 51.1 | 45.8 | 45.5 | 51.0 | 0.8 | 0.6 |
| **4c** | 28.6 | 24.4 | 36.1 | 33.9 | 1.0 | 0.4 |
| **4d** | 52.5 | 47.9 | 56.2 | 54.1 | 0.8 | 0.4 |

These trends can be explained as follows: A) The existence of the very poorly emissive charge-transfer transition decreases the overall quantum yields of derivatives **4a** and **4c**. B) More polar solvents favor the charge-transfer transition and therefore the quantum yield drops upon increasing the polarity from MCH/*n*-Hex to $CHCl_3$/DCM, for derivatives **4a** and **4c**, whereas the emission of the compounds without CT is almost unaffected. C) As the quantum yield of all molecules is equally quenched in MeOH and MeCN, a different molecular characteristic, common to all molecules must account for this phenomenon. Due to the fact that the solvent practically has no effect on the absorption spectra ($\rightarrow$ to which the character of ground state and excited state contribute), this behavior can only originate from different processes in the excited state.

## References


1. *APEX3* (**2016**), *SAINT* (**2015**) and *SADABS* (**2015**), Bruker AXS Inc., Madison, Wisconsin, USA.
2. Sheldrick, G. M., *SHELXT – Integrated space-group and crystal-structure determination*, *Acta Cryst.,* **2015**, *A71*, 3-8.
3. Sheldrick, G.M., *Crystal structure refinement with SHELXL*, *Acta Cryst.*, **2015**, *C71 (1)*, 3-8.
4. J. Li, C. G. Daniliuc, G. Kehr and G. Erker, *Angew. Chem. Int. Ed.*, 2019, **58**, 6737-6741.
5. D.F. Eaton, *Pure & Appl. Chem*, 1988, **60**, 1107-1114